Int J Adv Manuf Technol (2016) 83:1409–1418
DOI 10.1007/s00170-015-7671-4

ORIGINAL ARTICLE

Experimental investigation on fabrication of Al/Fe bi-metal tubes by the magnetic pulse cladding process

Zhisong Fan[1] · **Haiping Yu**[1,2] · **Fanchen Meng**[1] · **Chunfeng Li**[1,2]

Received: 22 December 2014 / Accepted: 3 August 2015 / Published online: 14 August 2015

Abstract Magnetic pulse cladding (MPC), a new technology, is proposed in this study to fabricate often utilized bi-metal tubing in engineering applications with an outer tubular component consisting of structurally strong material and an inner tubular layer of corrosion-resistant material. The MPC process includes an innovative feature that allows the outer and inner tubes to electromagnetically bond together by a sequential expansion process to form a mechanical bond between the tubes at the interface. The MPC process was experimentally arranged to produce an Al/Fe bi-metal tube with an outer carbon steel tube and an internal aluminum tube. A mechanical test was then applied to characterize bonding strength of the Al/Fe bi-metal tube. Significant process parameters including discharging voltage, radial gap, and feeding length were identified based on bonding strength influence. Overall feasibility was demonstrated for the MPC process in electromagnetic expansion pattern in the production of bi-metal tubing.

Keywords Bi-metal tube · Magnetic pulse cladding · Bonding strength · Al/Fe

1 Introduction

Steel tubes are utilized extensively in a range of industrial fields with considerable demand existing for tubular engineering components clad on outer or inner surfaces. Steel materials may be required to retain both sufficient mechanical strength and functional properties such as corrosion resistance depending on the application. Stainless steel features these characteristics, thus is often employed; however, it is somewhat inferior in strength, contributes to heavy construction, and results in higher costs. Two different metals then are combined to override deficiencies as a steel tube may be clad with the materials such as aluminum, titanium, and stainless steel suitable for using in corrosive environment. The thin cladding layer is in contact with the corrosive medium while the less expensive steel provides the strength and durability [1, 2].

Bi-metal tubes may be approximately divided into two categories according to the dominating bond mechanism: metallurgical bonding and mechanical bonding. Hot rolling is a classical technique applied to produce metallurgical-bond bi-metal sheets, which are utilized to fabricate seamed composite tubes [3]. Other methods to form metallic bonds include explosive welding [4], centrifugal casting [5], hot extrusion [6, 7], and spinning process [1, 8]. High temperature is often required for the attainment of metallic bonds, adding complications and inefficiency. Metallic bonds are typically needed only for severe service conditions (e.g., heat exchangers utilized for high temperature) while mechanical bonds are preferable when demands like high temperature are not present. Methods for mechanical bonding include the thermal shrink-fit method, thermo-hydraulic fit method [9], and hydraulic expansion method [10]. Low bonding strength and low work efficiency (due partly to the complex control operating system) operate as challenges for these methods.

Electromagnetic forming (EMF) is a high-speed, contact-free forming process employing a pulsed magnetic field to apply pressures on metal workpieces with high electrical conductivity, such as aluminum and magnesium [11–13]. A recent detailed review by Psyk et al. [14] showed the EMF

✉ Haiping Yu
haipingy@hit.edu.cn

[1] School of Materials Science and Engineering, Harbin Institute of Technology, Harbin, China

[2] National Key Laboratory for Precision Hot Processing of Metals, Harbin, China

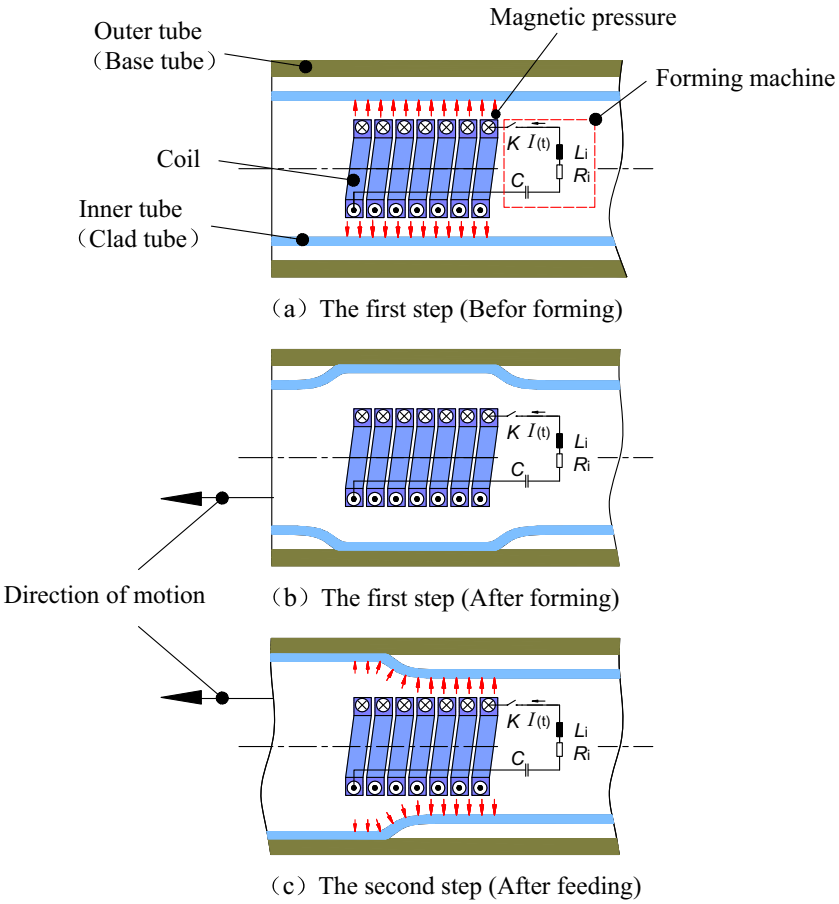

Fig. 1 Schematic diagram of the MPC process: **a** the first step (before forming), **b** the first step (after forming), **c** the second step (after feeding)

process has several advantages in comparison to conventional quasi-static forming processes, such as increased formability, high production rates, and high repeatability. Psyk et al. [14] pointed out that tubular components can be expanded or compressed by the EMF process, depending on the arrangement of coil and workpiece. In addition to forming operations, the EMF process can also be applied to join dissimilar materials promising significant potential for improved accuracy, reliability and environmental safety as discussed by Psyk et al. [14], Mori et al. [15], and Groche et al. [16]. Resulting connections generated by EMF can be classified into interference-fit joints, form-fit joints, and welded joints according to Weddeling et al. [17]. All three mechanisms and all possible combinations of the mechanisms can be utilized for profile-shaped workpieces according to Psyk et al. [14]. The connection for interference-fit joints is based on a difference in the elastic recovery of the joining partners, leading to a contact pressure between the parts after deformation, as presented by Mori et al. [15]. Marré et al. [18] investigated the processes of joining aluminum profiles to lightweight frame structures utilizing electromagnetic compression. Achievable interference-fit joint strength was found sufficient to transmit axial loads while the ability to form joint strengths within yield strength range of the weakest joining partner was also achieved. Geier et al. [19] reported on the interference-fit joining of aluminum-alloy AA6082 tubes with mandrels composed from different metallic and polymeric materials by electromagnetic compression. Their research work demonstrated that strength of the joint and the associated failure mechanisms direct related to process parameters and materials. Barreiro et al. [20] investigated influence of tube compressing velocity and joint material of the inner partner on the interference-fit joint produced

Fig. 2 The expansion coil for the magnetic pulse cladding process

Table 1 Mechanical properties of the tubes

Material	Yield strength σ_s (MPa)	Ultimate strength σ_b (MPa)	Elasticity modulus (GPa)
Aluminum alloy AA3003	79	118	67.5
Mild steel 1020	329	510	206

by electromagnetic compression. Joints produced by EMF were shown to resist axial forces as high as the tube yield strength and higher levels of pull-out load were achievable with the same impact velocity by increasing strength or stiffness of the mandrel material.

Studies introduced above demonstrated that joining by EMF is a cold, rapid, and reliable process, particularly valid for hollow tube joining. The joining process by EMF was constrained, however, to a small length of tubular components within the previous studies. Application of joining by EMF to longer tubes is limited due to the ultra-high mechanical strength of the EMF coil and the absence of sufficient energy that may be provided by an advanced forming machine. Development of a pulsed magnetic joining technique to fabricate larger length scale tubular components remains a challenge.

In this work, a novel cladding technique, magnetic pulse cladding (MPC), is developed to fabricate bi-metal tubes based on the electromagnetic tube expansion process. Experiments were conducted to clad the inner surface of carbon steel tube with aluminum alloy tube. Bonding strength of the prepared clad tube was measured through the compression-shear test, and effects of the main process parameters on bonding strength of the Al/Fe bi-metal tubes were reasonably evaluated. Feasibility of MPC in electromagnetic expansion pattern to fabricate bi-metal tubes was demonstrated. Results of the present work describe fabrication of bi-metal tubes though the main findings hold relevance for other types of multi-material structures, including applications of cladding adjoining edges of tubes for corrosion protection.

2 Experimental procedure

2.1 Principle and apparatus

The new proposed cladding process is schematically presented in Fig. 1 and consists of multi-steps conducted sequentially. Herein, the forming machine is symbolized by the capacitor C, the inner resistance R_i, and the inner inductance L_i (Fig. 1a). The process works, in each cladding step, by discharging a capacitor bank into a solenoid coil placed inside a clad tube. The sudden discharge of the capacitor by the closure of high voltage switch K produces a damped sinusoidal current $I(t)$ flowing through the coil, establishing a pulsed magnetic field in the vicinity. According to Faraday's law of induction, a current is induced in the clad tube which is directly opposed to the coil current, shielding the magnetic field in the gap between the coil and the clad tube. Energy density of the magnetic field leads to radial magnetic pressure acting orthogonally on the inner surface of the clad tube wall. Resulting

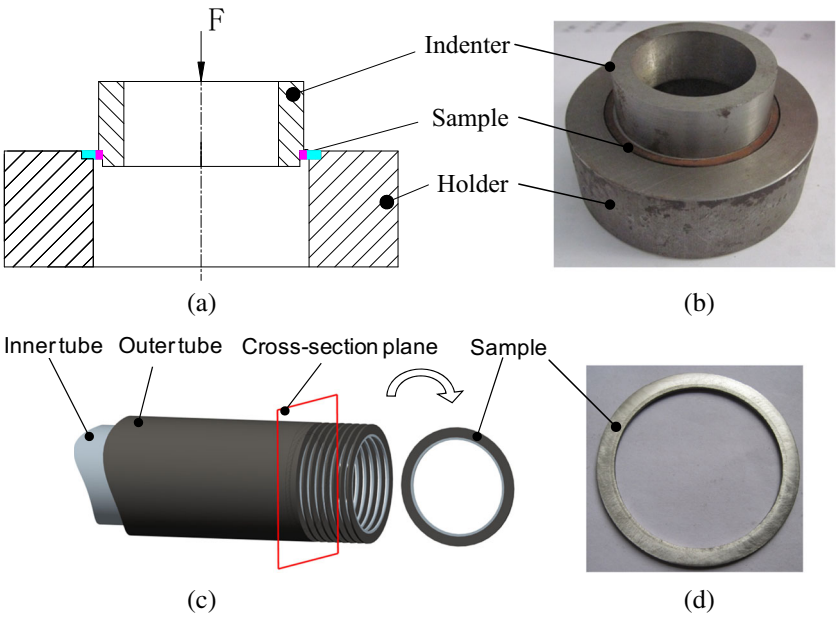

Fig. 3 The compression-shear test: **a** schematic illustration of a compression-shear test; **b** arrangement for measuring the shear strength; **b** sampling portion of the clad tube cut by WEDM; **d** a sample for the compression-shear test

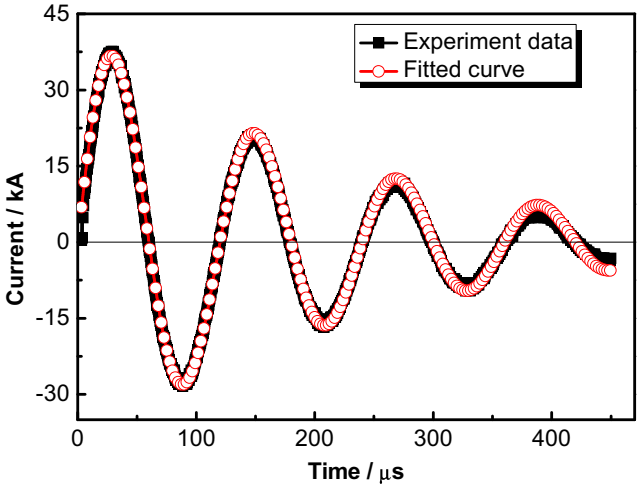

Fig. 4 Measured coil current profile

pulsed magnetic pressure then triggers radial plastic deformation as the clad tube yield strength is exceeded. Clad tube expansion occurs at sufficiently high velocity, creating a collision with a base tube which deforms elastically and, as a result, an interference-fit joint can be obtained in a way that both inner and outer tubes recuperate elastically.

Following completion of the first cladding step, both the inner and outer tubes are in motion in the axial direction with a feeding length for the second cladding step. The adjacent area of the clad tube is subjected to magnetic force in the second step (Fig. 1c), producing another overlap joint. A bi-metal tube with a desired length then can be obtained for several consecutive cladding steps.

Advantages of the proposed cladding process may be as follows:

- Capacity is achieved for manufacturing an internally clad tubular product with a long length while the electromagnetic forming machine stores only a relative small amount of energy.
- Compared to other cladding processes with mechanical contact between die and clad tube, the non-contact joining/cladding process results from plastic deformation of clad tubing, eliminating requirements for lubricants as no surface scuffing occurs and no other surface finish damages are generated.

Parameters of the radial gap between the clad and base tube, discharging voltage, and feeding length were considered in the experiment design for this study to investigate effects on bond strength.

Table 2 Parameters of electromagnetic forming system

$L(H)$	$\beta\ (s^{-1})$	ω (rad/s)
$3.648\times\ 10^{-6}$	4.48×10^{3}	5.236×10^{4}

The cladding experiments were carried out on a forming machine which has a capacitor of 100 μF and a maximum stored energy of 20 kJ. The expansion coil has 23 turns distributed over a length of 115 mm (L). Figure 2 shows a photograph of the coil for the magnetic pulse cladding process.

2.2 Materials and specimens

The investigation was performed on mild steel tube with an outer diameter of 60 mm and varied thicknesses from 2.5 to 4.2 mm. Aluminum alloy AA3003 was used as the clad layer. The aluminum tube has an outer diameter of 50 mm and a wall thickness of 1.2 mm. The length of both tubes is 270 mm. The stress–strain curves of the tube materials were determined by means of tensile tests carried out at room temperature. The mechanical properties of the aluminum and steel tubes are shown in Table 1. The inner surface of steel tube was machined to adjust the radial gap between the tubes. Prior to the assembly of two tubes, the inner surface of the steel tube and the outer surface of the aluminum tube were mechanically brushed and degreased with acetone. In order to assemble the tubes in co-axially aligned position, two polyvinyl chloride insulator rings with a length of 10 mm were inserted into the gap between the tubes at both ends. In addition, four holes were bored at both ends of steel tube for the escape of gas trapped in the gap.

2.3 Measurement of the bonding strength

To evaluate the bonding strength, an axial compression force leading to an interfacial shearing is applied on a sample (see Fig. 3a). Samples with thickness of 2 mm were cut longitudinally using wire electric discharge machining (WEDM) on the target zone of the prepared bi-metal tube specimen, as illustrated in Fig. 3c. The compression-shear tests were performed using an Instron-type tester under a speed of 0.5 mm/s at room temperature. Once the compression-shear test was completed, force–displacement curves were plotted for each sample and used to determine the maximum bonding force. Bonding strength can be obtained by dividing the force by the contact area of the double-layer ring sample. This relationship is expressed as:

$$\sigma_\tau = \frac{F_{\max}}{A} = \frac{F_{\max}}{\pi d h} \tag{1}$$

where σ_τ is the bonding strength in MPa, $F_{\max}$ is the maximum compression force in the force–displacement curve, and A is the contact surface given by the inner circumference of the outer tube πd times thickness h.

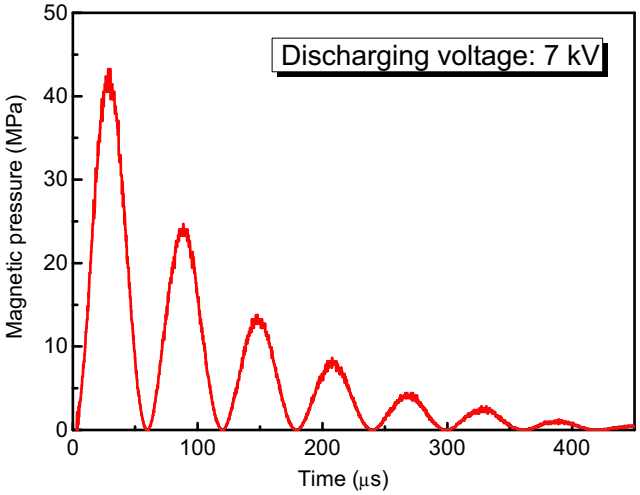

Fig. 5 Typical magnetic pressure pulse for discharging voltage of 7 kV

3 Results and discussion

3.1 Process characteristics of magnetic pulse cladding

Coil current was first measured utilizing a Rogowski probe to evaluate discharging parameters. Figure 4 shows the measured discharging current at a relative small discharging voltage of 7 kV. The discharging current is approximately described by the following formula:

$$I(t) = \frac{U_0}{\omega L} e^{-\beta t} \sin(\omega t) \tag{2}$$

where U_0 is the initial discharging voltage, ω is the angular frequency, L is the equivalent inductance of the system, and β is the damping exponent. Table 2 illustrates the obtained specific values of parameters. Measured discharging current is applied to estimate the magnetic pressure applied on the aluminum tube. If the magnetic field intensity on the aluminum tube's outer surface is approximately zero during the tube electromagnetic forming process, the magnetic field strength may be approximated with the following equation [14]:

$$H(t) = \frac{nI(t)}{l} k_H \tag{3}$$

where H is the magnetic field strength in the gap between the coil and clad tube and n the number of turns of the coil, $I(t)$ is the coil current, l is the coil length, and κ_H is the distribution coefficient. The magnetic pressure acting on clad tube can be estimated as:

$$P_{\text{mag}}(t) = \frac{1}{2} \mu H^2(t) \tag{4}$$

where μ is the permeability and H is the magnetic field strength in the gap between the coil and clad tube. From Eq. (2) to Eq. (4), it can be seen that the magnetic pressure

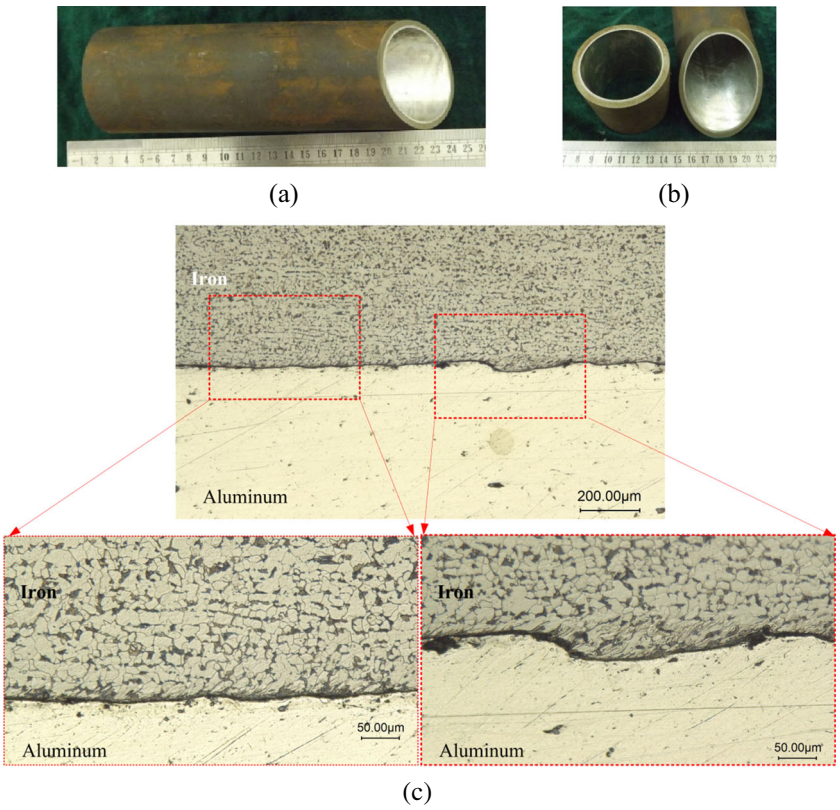

Fig. 6 Al/Fe bi-metal tube specimen prepared by MPC: **a** the sample, **b** the cutting edge of the sample, and **c** the interfacial region

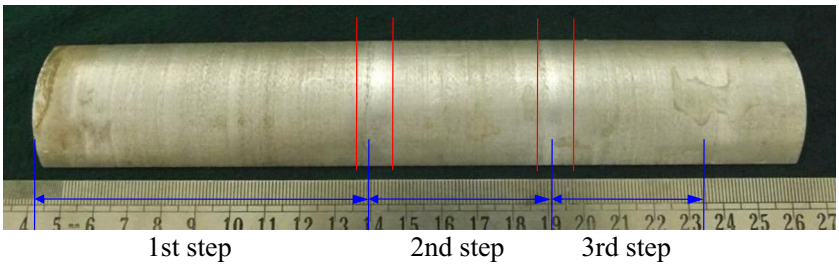

Fig. 7 The outer surface of the aluminum tube cut longitudinally from the two-layer Al/Fe tube

depends on the initial charging voltage. Typical profile of the magnetic pressure is shown in Fig. 5.

Deformation is typically completed during the first half-wave of the current, and, correspondingly, the magnetic pressure pulse [14]. Therefore, time for a single clad step can be estimated for completion within the range of microsecond. The entire process for fabricating a bi-metal tube with length of 300 mm may be completed within 90 s under the experimental conditions: 20 s for the manual feeding process and 8 s for the capacitor charging process. Overall cycle time of the MPC process would be reduced with automatic feed of tube assembly.

Figure 6 presents an Al/Fe bi-metal tube specimen (with appearance of a sound inner surface) prepared in three steps by MPC under conditions of 10 kV discharging voltage, 1.0 mm radial gap, and feeding length of 50%L (L denotes coil length). Figure 6c displays optical micrographs of the interfacial region from a cross-direction sectional cut with no welding evidence present.

The bi-metal tube was examined with the as-prepared sample cut in a longitudinal direction of the tube's axis. Separation of the inner and outer layers was observed, indicating the layers were bonded mechanically. Uniform deformation of the overlap portions was found to be fulfilled by the MPC process, while the outer surface of a separate aluminum layer was distinguished by a transition zone (Fig. 7). A trace of the inner machined surface of the steel tube was imprinted on the outer surface of the aluminum tube, indicating the aluminum tube collides violently with the base tube. No trace was left, however, by the transition zone. Approximately 10 mm in axial length, the transition zone is an area next to the joining area formed in the previous clad step and is schematically illustrated in Fig. 8. The slight collision of the transition zone with the base tube is primarily due to a change in the radial gap between the coil and aluminum tube. Larger radial clearance results in lower energy density of the magnetic field, thus, lower magnetic pressure. Homogeneity of the joint formed at different steps can be identified over the entire length of the bi-metal tube except the transition zone. Default samples utilized for assessment of the mechanical quality are then selected from the homogeneous area while joint quality in the transition zone will be discussed in "Effect of the feeding length on the bonding strength in the transition zone" section.

The load–displacement curve resulting from mechanical testing allows characterization of clad joint mechanical behavior. The joining area cut in cross-section by WEDM is illustrated in Fig. 9 while Fig. 10 presents a typical force–displacement curve obtained with a sample. An approximate linear increase with displacement prior to reaching peak value is demonstrated by the force. The curve decreases gradually following the sliding, and maximum force was defined as the criterion force to slip off. Process variance analysis will be

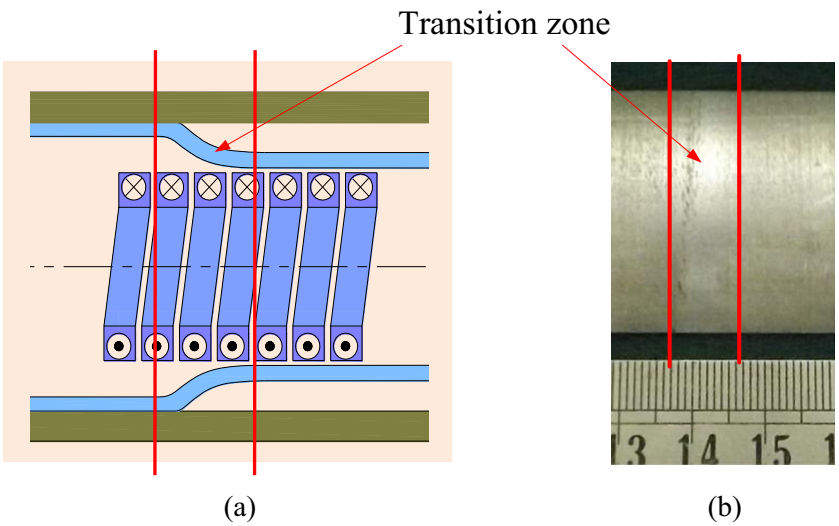

Fig. 8 The transition zone: **a** the schematic of the connection area formed between the steps and **b** the width of the transition zone in an Al/Fe bi-metal tube

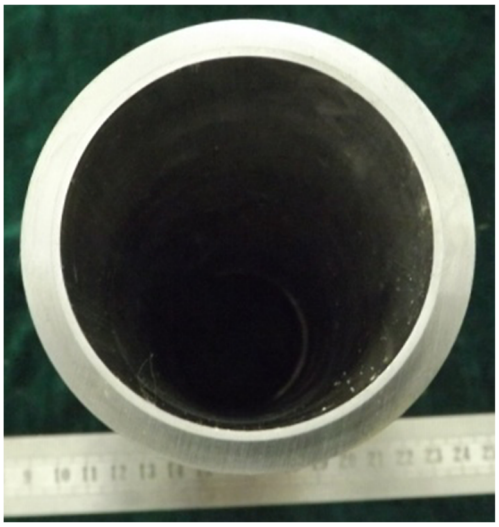

Fig. 9 Cross-sectional views of the two-layer tube

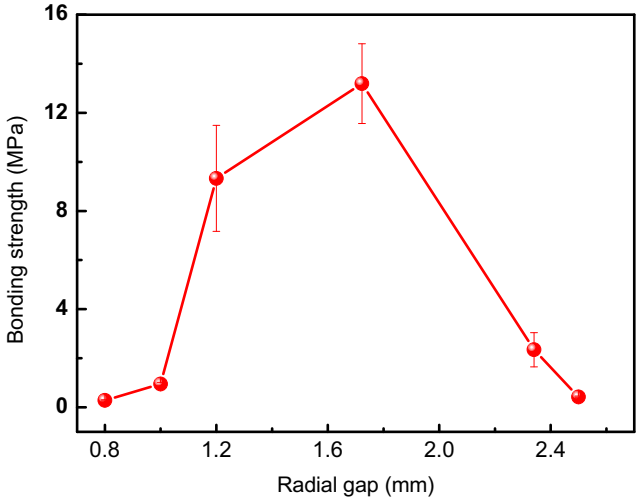

Fig. 11 Influence of the radial gap on the bonding strength

based on bonding strength in the following sections to provide further insight into methods for defining a useful parameter range.

3.2 Effect of the radial gap on the bonding strength

Influence of radial gap between the clad and base tube on the bonding strength was investigated with discharging voltage of 10 kV and feeding length of 57.5 mm (50%L). Radial gaps were selected varying in the range of 0.8–2.5 mm. Results of the compression-shear testing are presented in Fig. 11, demonstrating bonding strength versus radial gap. Thereby, with increasing initial gap, the bonding strengths first increase, show a maximum, and then decline. This behavior is similar with the results observed by [20] at electromagnetic compression. Evolution of the bonding strength demonstrates a maximum value of 13.19 MPa at a radial gap of 1.7 mm.

Dependency of the bonding strength's distribution on the radial gap can be attributed to flyer tube requirements for retaining a degree of radial gap for acceleration to achieve high impact velocity. According to Johnson [21], an impact pressure, $P_{\text{collision}}$, develops when two solid bodies collide at an impact velocity V_{impact}, and the relation between the collision pressure and the impact velocity is expressed as:

$$P_{\text{collision}} = \frac{\rho_1 C_1 \rho_2 C_2}{\rho_1 C_1 + \rho_2 C_2} V_{\text{impact}} \tag{5}$$

where ρ is the material density, C is the longitudinal wave speed, and V_{impact} is the impact velocity. The collision pressure deforms the base tube at the moment of impact. According to Eq. (5), it is found that an impact pressure of 500 MPa is generated for an impact velocity of 50 m/s for aluminum–steel couple [22].

The radial gap between the inner and outer tubes is among key parameters for obtaining high velocity. Contrasting with the hydraulic pressure expansion process, the energy transferred by the magnetic pressure pulse is not immediately transformed into plastic work during the tube electromagnetic expansion process. A large portion of the energy is initially stored as kinetic energy in the flyer tube (the inner tube). The flyer tube then further deforms after unloading the magnetic pressure pulse due to the release of previously stored kinetic energy. Figure 12 illustrates magnetic pressure of the first period, where P_{mag} represents magnetic pressure pulse and P_{yield} represents the so-called collapse pressure causing yield of a tube. Illustrated by the shaded area marked with a positive symbol, the impulse contributes to the kinetic energy of the flyer tube. Impact velocity is obviously dependent on magnetic pressure amplitude (correspondingly, the charging energy) while advantageous high-speed impact may be achieved through radial gap design within a certain range of values. Radial velocity of the flyer varies with distance within the radial gap for a given discharging energy. The flyer tube undergoes acceleration to a certain maximum velocity and subsequently undergoes deceleration. The flyer tube

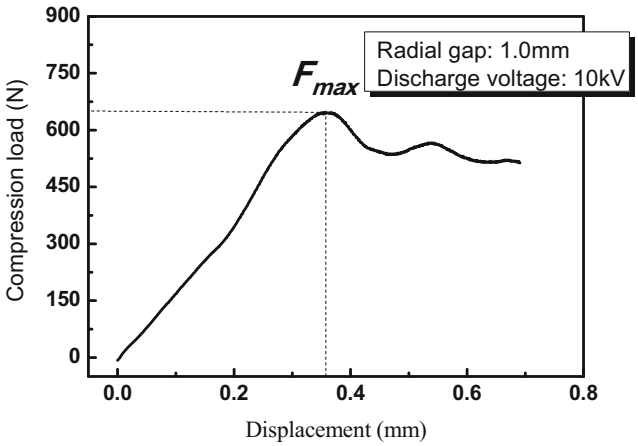

Fig. 10 Curve of compression load versus displacement

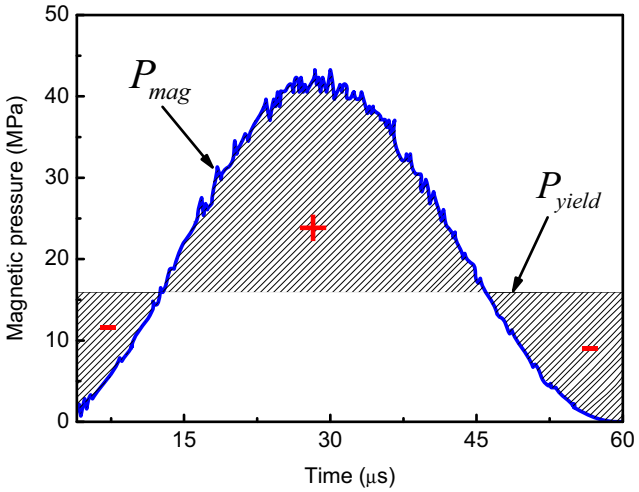

Fig. 12 A sketch of the magnetic pressure in the first half period

experiences a velocity change for exceptionally large radial gap that progressively increases to a maximum, decreasing to zero without the impact of both parts. Low radial gap does not allow sufficient acceleration as the flyer tube contacts with the base tube and radial velocity is then inadequate. Critical distance is therefore required to allow the flyer tube to impact the base tube with maximum velocity, thus increasing the collision pressure.

3.3 Effect of the charging voltage on the bonding strength

Experimental tests for assessing the effect of charging voltage on bonding strength were conducted with radial gaps of 2.3 and 2.5 mm under conditions with feeding length of 57.5 mm and investigated charging voltages varying from 9 to 12 kV by increments of 1 kV. Threshold discharge voltage for effective bonding was discovered to be approximately 10 kV with no bonds created under conditions with discharging voltage less than 10 kV. Figure 13 presents sample results at different discharging voltages for a radial gap of 2.3 mm. Figure 14 presents the effects of the discharge voltage on the bonding strength. Findings indicate, as expected, increased bonding strength with increase in discharge voltage. No bond was observed, however, under discharging voltage of 12 kV and radial gap of 2.3 mm. Distribution of bonding strength, depending on the discharging voltage, clearly illustrates an optimum value of 11 kV for both radial gaps.

Increase of charging voltage results in an increase of magnetic pressure applied on the flyer. Higher charging voltage leads to higher amplitude of the magnetic pressure, thus contact pressure increases for a constant radial gap at the moment of impact. Weakness of the bonding strength for the discharging voltage of 12 kV could be attributed to plastic deformation of the outer steel tube. The inner diameter of the steel tube, with a radial gap of 2.3 mm and discharging voltage of 12 kV, becomes 54.64 mm, while the outer diameter of the aluminum tube is only 54.62 mm following the collision. According to Eq. (5), pressures large enough to produce extensive plastic deformation are easily developed while undergoing impact. Once plastic deformation of the outer steel tube takes place, much of the energy dissipation occurs. Additionally, the bounce-back response of the flyer tube may also occur. Bounce-back response due to higher impact intensity is a common occurrence in impact processes [23, 24], thus stiffness of the outer tube should be considered to obtain an optimal mechanical bond between the tubes.

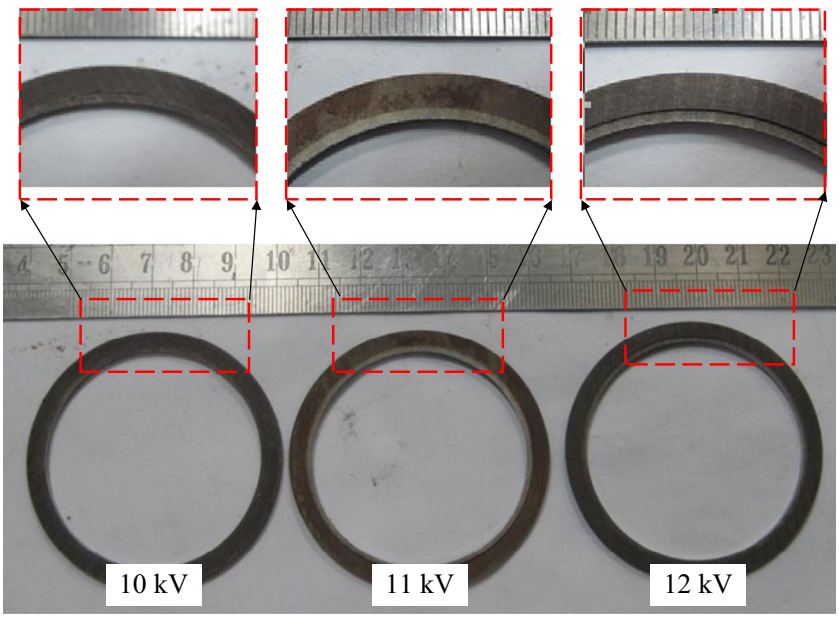

Fig. 13 Samples for compression-shear test formed under different discharging voltages for a constant radial gap of 2.3 mm

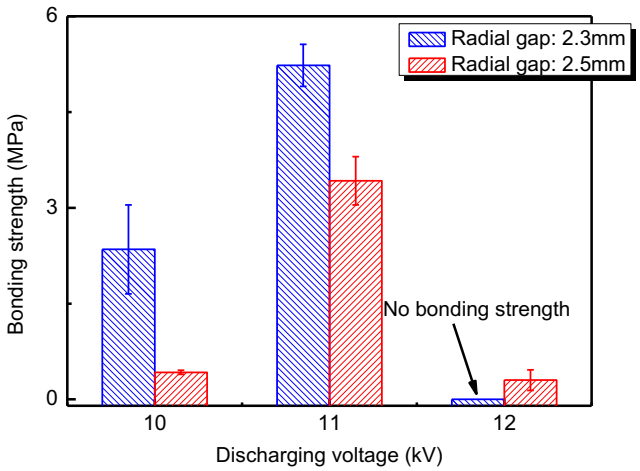

Fig. 14 Influence of discharging voltage on the bonding strength

3.4 Effect of the feeding length on the bonding strength in the transition zone

A typical characteristic of the magnetic pulse cladding process is the transition zone, as discussed in "Process characteristics of magnetic pulse cladding" section. Further experiments were conducted to study the effect of feeding length on bonding strength in the transition zone under conditions with discharging voltage of 10 kV, radial gap of 1.5 mm, and feeding length varying from 57.5 mm (50%L) to 115 mm (100%L). Five samples were cut in succession from the transition zone and a mean value of the bonding strength was applied. Figure 15 illustrates the bonding strength versus feeding length. Bonding strength of the transition zone increases from 0.28 to 1.78 MPa by shortening the feeding length from full to half of the coil length. Bonding strength increase could be attributed to the improvement of magnetic field distribution in the transition zone. According to Yu et al. [25], magnetic force distribution is inhomogeneous due to the end effect of a coil and the magnetic force varies from a peak value in the center to a minimum in both ends of the coil. A more intense magnetic pressure pulse may be obtained when the center of the coil is located closer to the transition zone.

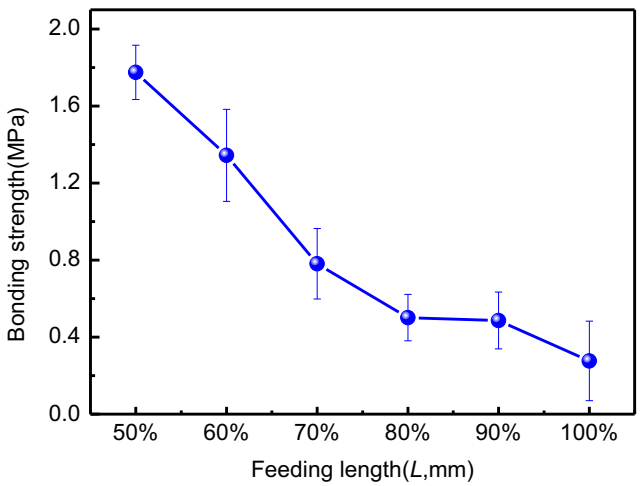

Fig. 15 Influence of the feeding length on the bonding strength

Compared to bonding strength (about 12 MPa) in the non-transition zone ("Effect of the radial gap on the bonding strength" section), maximum bonding strength in the transition zone with the feeding length of 50%L is relatively small, possibly attributed to specific configuration of the transition zone. Magnetic pressure applied in the transition zone is smaller than that in the non-transition zone due to the varied radial gap between the coil and clad tube. It is also worthy to note that feeding length may be properly increased for efficiency with minimal loss in bonding strength as axial length of the transition zone is a relatively small fraction.

4 Conclusions

Magnetic pulse cladding (MPC), a novel cladding technology, is developed in this study to fabricate bi-metal tubes. The MPC process is based on a sequential electromagnetic expansion process. The experimental investigation of the MPC process reaches the following conclusions:

1. The proposed magnetic pulse cladding process is feasible in the fabrication of bi-metal tubes with a mechanical bond.
2. Radial gap between the clad and base tubes strongly affects bonding strength resulting from the impact-based process. Required impact velocity is not attained at radial gaps that are too low or large, thus bonding strength may be optimized by varying initial radial gap between specific thresholds to achieve the maximum impact velocity. The adequate radial gap producing maximum bond strength of 13.19 MPa was established at a radial gap of 1.7 mm for a constant discharging voltage of 10 kV.
3. Bonding strength of the clad samples increases with discharging voltage due to increasing peak values of the pulsed magnetic pressure. Plastic deformation of the outer steel tube alters this tendency and stiffness of the outer tube should be considered to obtain an optimal mechanical bond between the tubes.
4. The transition zone with axial length of approximately 10 mm functions as a significant process characteristic. Bonding strength in the transition zone is weak compared to other regions and can be improved by shortening the feeding length. Maximum value can be obtained with feeding length at half of the coil length.

Acknowledgments The authors gratefully acknowledge both the National Natural Science Foundation of China (grant no. 51475122) and National Basic Research Program of China (973 Program) [2011CB012805] for their kind financial support of this work.

References

1. Mohammad SM, Abbas A (2011) Fabrication of copper/aluminum composite tubes by spin-bonding process: experiments and modeling. Int J Adv Manuf Technol 54:1043–1055
2. Zhan Z, He Y, Wang D, Gao W (2006) Cladding inner surface of steel tubes with Al foils by ball attrition and heat treatment. Surf Coat Technol 201:2684–2689
3. Henryk D, Maciej P (1983) On the theory of the process of hot rolling of bimetal plate and sheet. J Mech Work Technol 8(4): 309–325
4. Sun XJ, Tao J, Guo XZ (2011) Bonding properties of interface in Fe/Al clad tube prepared by explosive welding. Trans Nonferrous Metals Soc 21:2175–2180
5. Sponseller DL, Timmons GA, Bakker WT (1998) Development of clad boiler tubes extruded from bimetallic centrifugal castings. J Mater Eng Perform 7(2):227–238
6. Chen Z, Ikeda K, Murakami T, Takeda T, Xie JX (2003) Fabrication of composite pipes by multi-billet extrusion technique. J Mater Process Technol 137(1):10–16
7. Berski S, Dyja H, Maranda A, Nowaczewski J, Banaszek G (2006) Analysis of quality of bimetallic rod after extrusion process. J Mater Process Technol 177(1):582–586
8. Mohebbi MS, Akbarzadeh A (2010) A novel spin-bonding process for manufacturing multilayered clad tubes. J Mater Process Technol 210:510–517
9. Yoshida T, Mann T, Matsuda S, Matsui S, Atsuta T, Toma S, Itoga K (1981) The development of corrosion-resistant tubing. In: Proceedings of the 1981 OTC Annual Offshore Technology Conference, Houston 365–378
10. Wang X, Li P, Wang R (2005) Study on hydro-forming technology of manufacturing bimetallic CRA-lined pipe. Int J Mach Tools Manuf 45:373–378
11. Xu JR, Yu HP, Li CF (2013) Effects of process parameters on electromagnetic forming of AZ31 magnesium alloy sheets at room temperature. Int J Adv Manuf Technol 66:1591–1602
12. Cui XH, Mo JH, Han F (2012) 3D multi-physics field simulation of electromagnetic tube forming. Int J Adv Manuf Technol 59(5–8): 521–529
13. Xu JR, Cui JJ, Lin QQ, Li CF (2014) Effects of driver sheet on magnetic pulse forming of AZ31 magnesium alloy sheets. Int J Adv Manuf Technol 72:791–800
14. Psyk V, Risch D, Kinsey BL, Tekkayaa AE, Kleiner M (2011) Electromagnetic forming—a review. J Mater Process Technol 211:787–829
15. Mori K, Bay N, Fratini L, Micari F, Tekkaya AE (2013) Joining by plastic deformation. CIRP Ann Manuf Technol 62(2):673–694
16. Groche P, Wohletz S, Brenneis M, Pabst C, Resch F (2014) Joining by forming—a review on joint mechanisms, applications and future trends. J Mater Process Technol 214(10):1972–1994
17. Weddeling C, Woodward ST, Marré M, Nellesen J, Psyk V, Tekkaya AE, Tillmann W (2011) Influence of groove characteristics on strength of form-fit joints. J Mater Process Technol 211(5): 925–935
18. Marré M, Brosius A, Tekkaya AE (2008) Joining by compression and expansion of (none-) reinforced profiles. Adv Mater Res Flex Manuf Lightweight Frame Struct Phase II Integr 43:57–68
19. Geier M, José MM, Rossi R, Rosa PAR, Martins PAF (2013) Interference-fit joining of aluminum tubes by electromagnetic forming. Adv Mater Res 853:488–493
20. Barreiro P, Beerwald C, Homberg W, Kleiner M, Löhe D, Marré M, Schulze V (2006) Strength of tubular joints made by electromagnetic compression at quasi-static and cyclic loading. In: International Conference on High Speed Forming, Germany 107–117
21. Johnson W (1972) Impact strength of materials. Edward Arnold, London
22. Seth M, Vohnout VJ, Daehn GS (2005) Formability of steel sheet in high velocity impact. J Mater Process Technol 168(3):390–400
23. Xu JR, Cui JJ, Lin QQ, Li YR, Li CF (2014) Magnetic pulse forming of AZ31 magnesium alloy shell by uniform pressure coil at room temperature. Int J Adv Manuf Technol 77:289–304
24. Golovashchenko SF, Gillard AJ, Mamutov AV, Ibrahim R (2014) Pulsed electrohydraulic springback calibration of parts stamped from advanced high strength steel. J Mater Process Technol 214(11):2796–2810
25. Yu HP, Li CF (2007) Effects of coil length on tube compression in electromagnetic forming. Trans Nonferrous Metals Soc 17(6): 1270–1275